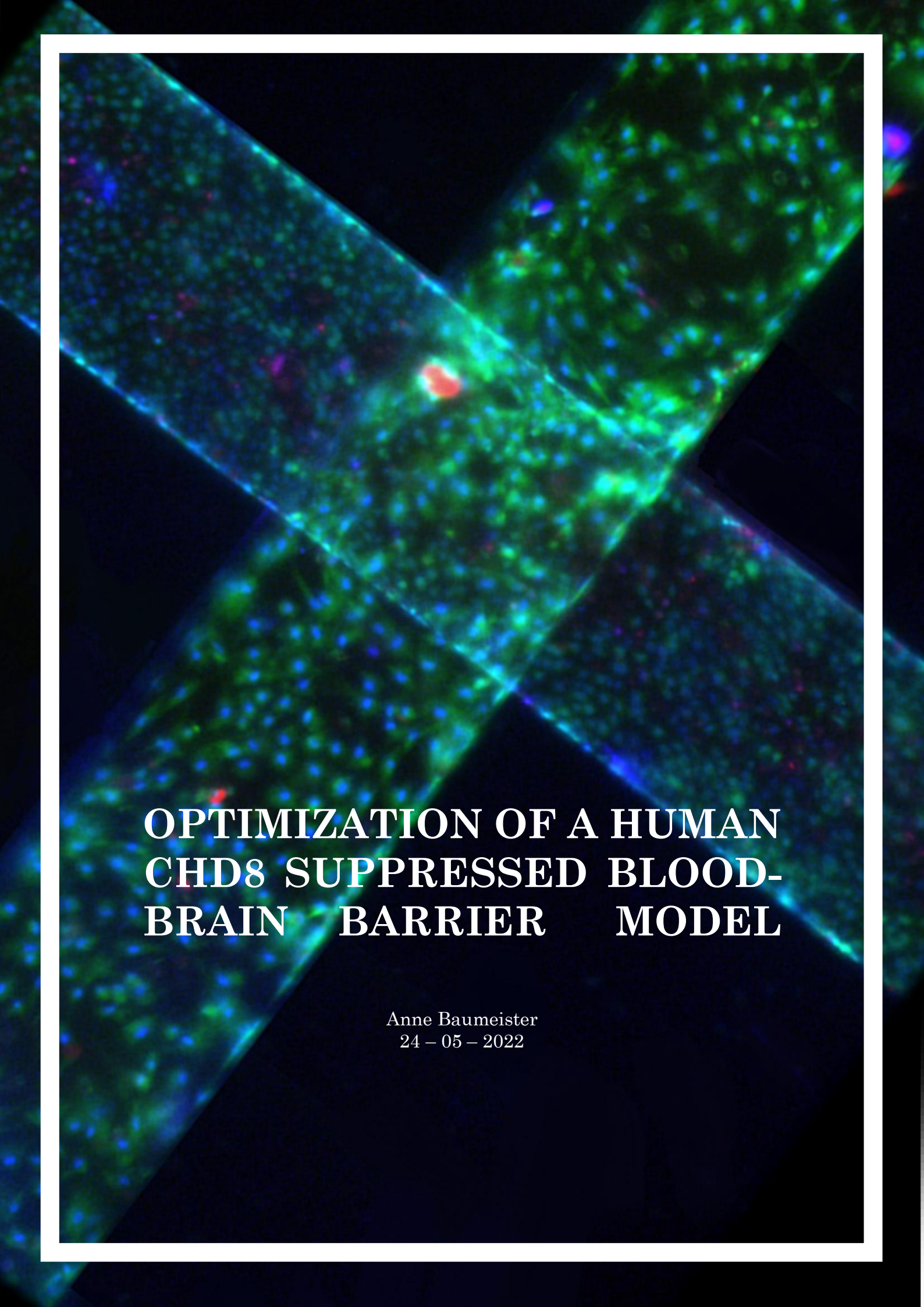

OPTIMIZATION OF A HUMAN CHD8 SUPPRESSED BLOOD-BRAIN BARRIER MODEL

Anne Baumeister
24 – 05 – 2022

OPTIMIZATION OF A HUMAN CHD8 SUPPRESSED BLOOD-BRAIN BARRIER MODEL

Anne Baumeister
S2013207
24 – 05 – 2022

Examination Committee:
Prof. Dr. Ir. Loes Segerink
Prof. Dr. Kerensa Broersen
Robin Pampiermole, MSc

Biomedical Engineering
Faculty of Science and Technology

ABSTRACT

An increasing number of children is being diagnosed with autism spectrum disorder (ASD), characterized by deficits in social communication and restrictive repetitive actions. 50 – 80% of ASD diagnosed children also experience sleep problems, which has a big impact on quality of life for both child and parent. A correlation is found in ASD diagnosed children between mutation of chromodomain-helicase-DNA-binding protein 8 (CHD8) and having sleep problems. Since it is known that the blood-brain barrier (BBB) is involved in sleep regulation, the goal of this research was to optimize a CHD8 suppressed BBB model to study barrier integrity.

Astrocytes and hCMEC/D3 were transfected with siCHD8 by transfection reagents RNAiMAX, Lipo2000, Viafect, and Dharmafect to test silencing efficiency. The integrity of a co-cultured cell layer was analysed with a permeability assay on transwells. PDMS chips were produced and seeded with astrocytes and hCMEC/D3. A live/dead assay was performed to analyse cell viability with and without siCHD8 transfection after 5 days of cultivation in chip.

Silencing of CHD8 in astrocytes was successful using transfection reagent RNAiMAX, while CHD8 suppression in hCMEC/D3 was observed with transfection reagents Viafect and Dharmafect. The permeability assay showed a high integrity of co-cultured hCMEC/D3, however, no conclusion could be drawn between CHD8 silenced and non-silenced cultures. After 5 days of cultivation, a high percentage of viable cells were analysed in chips with no harmful effect of siCHD8 transfection. In this research, a human BBB model was optimized by increasing CHD8 silencing efficiency, creating an integer co-culture barrier, and making a first step transforming a static transwell to a dynamic chip.

SAMENVATTING

Een toenemend aantal kinderen wordt gediagnosticeerd met autismespectrumstoornis (ASS), gekenmerkt door verminderde sociale vaardigheden en beperkende herhaalde handelingen. 50 – 80% van de kinderen gediagnosticeerd met ASS ervaart ook slaapproblemen, wat een grote impact heeft op de kwaliteit van leven van zowel het kind als de ouder. Bij kinderen met de diagnose ASS is een correlatie gevonden tussen mutatie van chromodomein-helicase-DNA-bindend eiwit 8 (CHD8) en slaapproblemen. Aangezien bekend is dat de bloed-hersenbarrière (BHB) betrokken is bij slaapregulatie, was het doel van dit onderzoek om een CHD8-onderdrukt BHB-model te optimaliseren om de integriteit van de barrière te onderzoeken.

Astrocyten en hCMEC/D3 werden getransfecteerd met siCHD8 door middel van de transfectiereagentia RNAiMAX, Lipo2000, Viafect, en Dharmafect om de silencing-efficiëntie te testen. De integriteit van samen-gekweekte monolagen werd geanalyseerd met een permeabiliteitstest op transwellen. PDMS-chips werden geproduceerd en gezaaid met astrocyten en hCMEC/D3. Een viabiliteitstest werd uitgevoerd om de levensvatbaarheid van de cellen te analyseren met en zonder siCHD8-transfectie na 5 dagen cultuur in een chip.

Onderdrukking van CHD8 in astrocyten was succesvol met transfectiereagent RNAiMAX, terwijl in hCMEC/D3 een CHD8-suppressie werd waargenomen met transfectiereagentia Viafect en Dharmafect. De permeabiliteitstest toonde een hoge integriteit van samen-gekweekte monolagen, maar er kon geen conclusie worden getrokken van het verschil in permeabiliteit tussen CHD8-gedempte en niet-gedempte culturen. Na 5 dagen kweek in chips, werd een hoog percentage levensvatbare cellen geanalyseerd zonder schadelijk effect van siCHD8-transfectie. In dit onderzoek werd een menselijk BBB model geoptimaliseerd door een toegenomen CHD8 silencing efficiëntie, het creëren van een integere co-cultuur barrière, en het maken van de eerste stap in het transformeren van een statische transwell naar een dynamische chip.

CONTENTS

LIST OF ABBREVIATIONS

2D	two-dimensional
3D	three-dimensional
ASD	autism spectrum disorder
AGM	astrocyte growth medium
BBB	blood-brain barrier
BECs	brain endothelial cells
Calcein-AM	calcein acetoxymethyl ester
CHD8	chromodomain helicase DNA-binding protein 8
CNS	central nervous system
DC	detergent compatible
DNA	deoxyribonucleic acid
ECM	extracellular matrix
ECs	endothelial cells
EGM	endothelial growth medium
EthD-1	ethidium homodimer-1
FBS	fetal bovine serum
FITC	fluorescein isothiocyanate
hAC	human astrocytes
hCMEC	human cerebral micro vessel endothelial cells
kDa	kilodalton
NVU	neurovascular unit
PBS	phosphate buffered saline
PDMS	polydimethylsiloxane
PFA	paraformaldehyde
PVDF	polyvinylidene fluoride
SDS-PAGE	sodium dodecyl sulphate polyacrylamide gel electrophoresis
Si	silicon
siNC	negative control silencer
siRNA	small interfering ribonucleic acid
TBS	tris buffered saline
TEER	trans endothelial electrical resistance
VE-cadherin	vascular endothelial cadherin
ZO-1	zonula occludens-1

INTRODUCTION

THE BLOOD BRAIN BARRIER

Nearly all functions of human body and mind are controlled by the central nervous system (CNS), consisting of the brain and the spinal cord. Among many other things, the CNS is responsible for our ability to understand, move, speak, remember, sense, digest, sleep, and breathe. [1, 2] For proper functioning, it is thus of major importance to protect these vital organs against harmful intruders. At the end of the 19th century, Paul Ehrlich and his student Edwin Goldman were the first to find out that a biological barrier existed at the blood-brain interface, effectively separating the brain and spinal cord from the rest of the body. By injecting a dye into the blood circulation of mice, they found out that it infiltrated all tissues except for the CNS and vice versa (*figure 1*). [3] The highly controlled physical interface between blood vessels and brain tissue is now known as the blood-brain barrier (BBB).

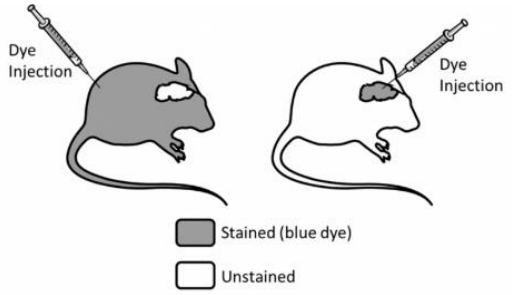

Figure 1: A schematic representation of the experiment Ehrlich and Goldman performed on mice. [4]

The BBB is a physical and enzymatic barrier, protecting the CNS by strict regulation of molecules between the peripheral blood and brain parenchyma, maintaining physical and chemical homeostasis of the neural microenvironment. [5, 6] Passage across the BBB is limited, because of its high trans endothelial electrical resistance (TEER) and low paracellular and transcellular permeability. [7, 8]

The integrity of the BBB is mediated by a multicellular system, in which brain endothelial cells (BECs) are centrally located in cylindrical shape. [9] BECs have unique properties compared to endothelial cells in the rest of the body, namely the absence of fenestrations, infrequent pinocytic vesicular transport, and more extensive adherens and tight junction proteins. [10-14] The abundancy of the latter is hugely important for barrier integrity, with the transmembrane protein vascular endothelial (VE-) cadherin being particularly important. [14] Studies show that endothelial monolayer permeability increases when suppressing VE-cadherin. [13] VE-cadherin also upregulates

claudin-5, the key component of the tight junction strand, which in their place are linked to the cytoskeleton by zonula occludens (ZO) -1, -2, and -3. [15] Although, BECs act as the principal barrier unit, it is known that a surrounding network of molecular crosstalk between a variety of cell types is necessary for BBB formation and integrity maintenance. [9, 16]

Most part of the endothelial capillary wall is encircled by pericytes within a common basal lamina. They are closely connected to each other by gap junctions, focal adhesion plaques, and peg-and-socket-invaginations. [3, 17] Even though, little is known about the precise function of pericytes, multiple studies show their importance in developing and maintaining BBB integrity. [10, 18, 19] As an example, R. Bell *et al.* (2010) shows induced pathological BBB leakiness after pericyte loss. [19]

The most abundant cell type of the BBB are astrocytes. Their specialized end-feet cover nearly the entire surface of the outer layer of the endothelium. [10] Besides pericytes, astrocytes are also considered a major source for BBB barrier inducing and maintaining signals. S. Liebner *et al.* (2018) shows that astrocytes improve endothelial barrier function not only in co-culture models, but also in endothelial monocultures administrated by astrocyte conditioned medium, concluding that secreted factors are important for BBB integrity. [10, 20-22] However, since the mechanisms of these phenomena are not entirely understood, more research is required to unravel the complex molecular crosstalk between BECs, pericytes and astrocytes.

There is increased awareness that BBB function and dysfunction are mediated by complex interaction between a network of not only BECs, pericytes and astrocytes, but also neurons and glial cells. The interaction of these cells in steady state and their collective response to injury led to the theory that these cells form a functional unity together, called the neurovascular unit (NVU; *figure 2*). [7, 10, 23]

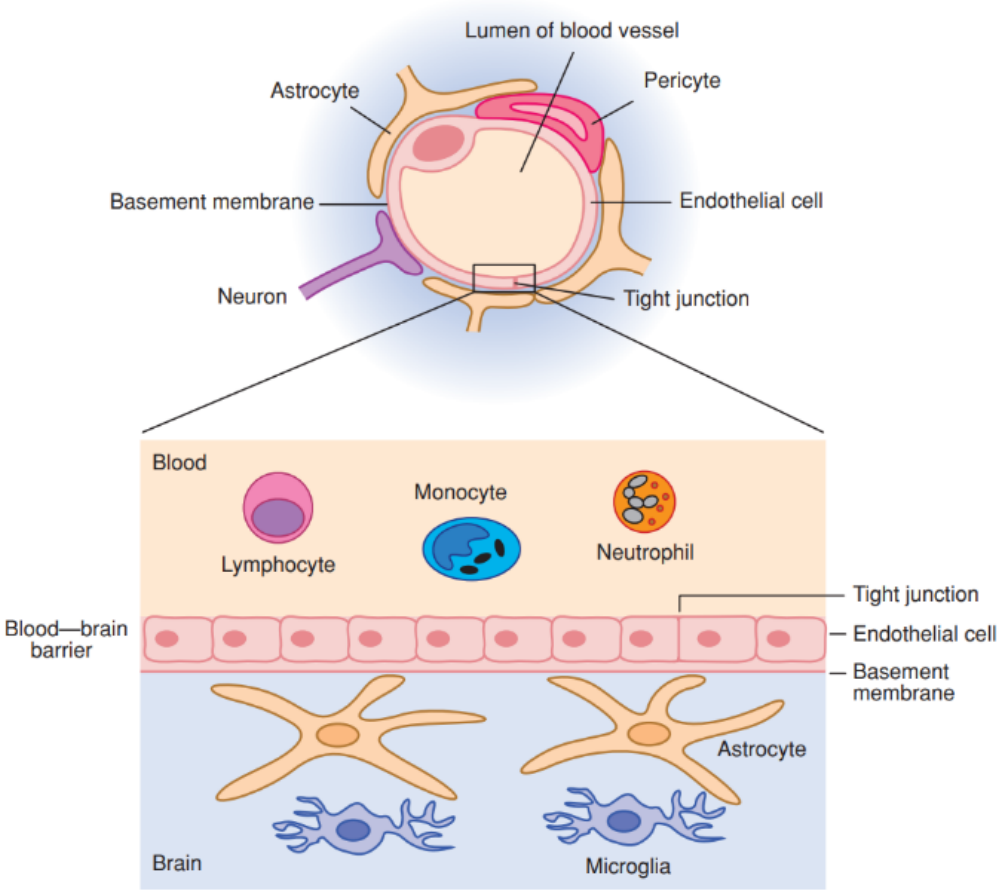

Figure 2: A schematic representation of the NVU. BECs, closely connected to each other by tight junction proteins, are surrounded by pericytes and astrocyte end-feed to form the BBB. Neurons and microglia also contribute to NVU functioning. [24]

AUTISM SPECTRUM DISORDER

The past decades, an increasing number of children are diagnosed with autism spectrum disorder (ASD), which is a neurodevelopmental disorder. [25, 26] Patients with ASD have a large variety of symptoms, but the most characteristics are deficits in social communication and restrictive repetitive actions in behaviour, activities and interests. [27 – 29] In addition to these core symptoms, 50 - 80% of ASD diagnosed children experience sleep problems, which includes problems falling asleep, staying asleep, reduced sleep duration, daytime sleepiness, and bedtime resistance. [26, 31, 32] This prevalence is 3 to 4 times higher compared to typically developing children. [29 – 31, 33, 34] All symptoms of ASD can be amplified by sleeping problems. Possible problematic effects are exhaustion, concentration problems, mood changes, memory problems and paranoia feelings. [32, 35] As a consequence of these symptoms, several studies show a correlation between sleep problems in children with ASD and higher parenting stress. [33, 36, 37] Even though sleep problems in ASD diagnosed children have a major impact on quality of life for both child

and parent, the mechanism underlying this phenomenon is poorly understood. [38, 39]

74 – 93% of ASD inducing factors are heritable, whereby attention is increased for specific determination of individual genetic mutations associated with ASD prevalence. [40, 41] De novo single-nucleotide mutations have been identified in dozens of genes that appear to contribute to ASD development, the most common mentioned called chromodomain helicase deoxyribonucleic acid (DNA) binding protein 8 (CHD8). [41, 42] Interestingly, in ASD patients with a CHD8 mutation, sleep problems occur frequently. [30 – 32] CHD8 is potentially important during brain development, and is especially expressed in the early prenatal period. [42] Studies indicate that CHD8 plays a crucial role in cortical development by promoting the proliferation of neural progenitors. By facilitation of neuron expression and division, an appropriate number of neurons generates in the brain. [43] Mutations in the CHD8 paralog chromodomain helicase DNA binding protein 7 (CHD7) lead to CHARGE syndrome, which is also a neurodevelopmental disorder. Even though, primary attention was given to physical symptoms, it is now well established that children with CHARGE syndrome also show ASD like features and sleep problems. [33, 44, 45] CHD8 and CHD7 interact with each other and are part of a complex unit that organizes chromatin assembly. The molecular interaction between CHD8 and CHD7 and the overlapping symptoms of ASD and CHARGE suggest that both disorders have a common mechanistic basis. [33] M. Coll-Tané *et al.* (2021) found a correlation between CHD8/CHD7 ortholog Kismet and ASD-associated sleep disturbances in *Drosophila*, and also shows a high expression of CHD8 and CHD7 in endothelial cells, pericytes, astrocytes, and glial cells, suggesting an essential role of CHD8 and CHD7 in the BBB. [33]

ORGAN-ON-CHIP

Animal models and two-dimensional (2D) *in vitro* cell culture platforms have been used for decades to study disease behaviour and drug effect. [46] Even though they contributed to a lot of medical knowledge, both also have evident drawbacks. For example, animal models are time-consuming, give ethical concerns, and cannot be translated to human conditions one-to-one. 2D *in vitro* cell culture platforms, consisting of a cell monolayer, fail to mimic the complex three-dimensional (3D) *in vivo* microenvironment in which cells interact with surrounded cells and extracellular matrix (ECM), essential for proper cell differentiation and functioning. [46 – 48] Recent development of 3D microfluidic organ models could overcome the disadvantages of animal and 2D *in vitro* models as rising platform for disease studies. These microfluidic organ models are known as organ-on-chip models. [50]

Organ-on-chip models provide many benefits to multiple areas in science and engineering, including the biomedical field. The main advantages of using these microfluidic devices are the reduced costs of sample and reagent due to reduction of necessary amount, fast detection, and availability to mimic the *in vivo* environment. [51]

A transwell model (*figure 3*) is used as a relatively simple set-up for an *in vitro* representation of specific organs. A transwell consist of two compartments, divided by a porous membrane, on which cells are cultured on both sides, creating a co-culture. For mimicry of the BBB, BECs are cultured as a monolayer on the apical side of the membrane, while other cells of the neurovascular unit are seeded on the basolateral side. The advantages of the use of a transwell model are its simplicity, moderate throughput and the ability to use human cell sources. The latter will circumvent probable translation problems to the clinic. [52, 53]

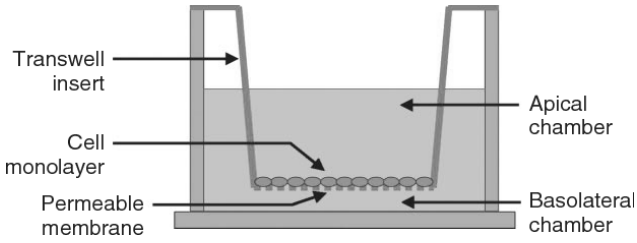

Figure 3: A schematic representation of a transwell model. [54]

Even though the transwell model is widely used as an *in vitro* co-culture platform, this simple set up fails to imitate key characteristics of the BBB, such as the neurovascular unit morphology and shear stress due to blood flow. [53] Involvement of such components has been shown to increase expression of adherens and tight junction proteins and decrease barrier permeability. Subsequently, increasing physiological accuracy will likely increase the predictive potential of BBB organ-on-chip models. Continuous advancements in microtechnology can lead to the creation of realistic *in vivo* like BBB models. [50] Nevertheless, increased physiological accuracy is directly associated with increased technical complexity. [55]

In this research, both the transwell and an organ-on-chip model with two channels perpendicular to each other are used with a co-culture of human cerebral micro vessel endothelial cells (hCMEC/D3) and human astrocytes (hAc). There are many different endothelial cell lines, but hCMEC/D3 are used because of their easy accessibility, simplicity and possession of BEC

characteristics. [56] The transwell model is used for simple analysation of hCMEC/D3 monolayer integrity, while the chip model is used to transform a static BBB model to a dynamic one. The chip is made of polydimethylsiloxane (PDMS), which is a transparent, easy to handle, quickly cross-linked, and relatively cheap material. [51]

THESIS OUTLINE

This research aims to optimize a CHD8 suppressed human BBB model for examination of barrier integrity in ASD diagnosed children with sleep problems.

The objectives include:

- Silencing of ASD associated CHD8 in astrocytes and endothelial cells
- Analysation of integrity of a CHD8 suppressed co-cultured monolayer
- Transformation of the static human BBB model in transwell to a dynamic model in chip for increased mimicry of *in vivo* situations

MATERIALS AND METHODS

CELL CULTURE

hCMEC/D3 (Merck Millipore) were cultured in endothelial growth medium (EGM; Cell Applications, Inc) on 100 μg ml^{-1} collagen-1 (rat tail, Corning) pre-coated culture flasks (Greiner, Austria) at 37°C and 5% CO_2. For all experiments, hCMEC/D3 with a passage number of 30 – 35 were used. Human astrocytes (Cell Applications, Inc) were cultured in astrocyte growth medium (AGM) with 0.2% fetal bovine serum (FBS), 0.1% penicillin/streptomycin solution, and 0.1% astrocyte growth supplements (ScienCell Research Laboratories) in culture flasks (Greiner, Austria) at 37°C and 5% CO_2. For the experiments, astrocytes with a passage number of 6 – 10 were used.

Prior to cell seeding on transwells or chips, the apical side of the membrane was coated with collagen-1 for 1 hour at 37°C and washed with phosphate buffered saline (PBS) afterwards. The transwells were seeded with 50 μL of $1 \cdot 10^5$ cells/mL astrocytes in AGM on the basolateral side of the membrane and incubated upside down at 37°C for 3 hours to allow attachment. To prevent dehydration, medium was added every 15 minutes. Subsequently, the transwells were inverted and placed in a 24-well plate with 600 μL AGM. After 16 – 24 hours of incubation, 100 μL of $1.5 \cdot 10^5$ cells/ml hCMEC/D3 in EGM was added to the apical side of the membrane. The co-culture was kept in 37°C and 5% CO_2 for 4 – 7 days to obtain a hCMEC/D3 monolayer. Medium was refreshed daily.
The chips were seeded with $2 \cdot 10^6$ cells/mL astrocytes in AGM in the bottom channel and incubated upside down at 37°C for at least 3 hours to allow attachment. Subsequently, the chips were inverted and pipet tips containing 200 μL fresh AGM were carefully placed in the in- and outlets. After 16 – 24 hours of incubation, $5 \cdot 10^6$ cells/mL hCMEC/D3 in EGM were seeded in the top channel. The co-culture was kept in 37°C and 5% CO_2 for 4 days. Medium was refreshed daily.

SICHD8 TRANSFECTION

CHD8 protein levels in hCMEC/D3 and astrocytes were suppressed using small interfering ribonucleic acid (siRNA). A siRNA mastermix consisting of 100 pmol mL^{-1} siCHD8 (ThermoFisher; cat. 4392420; ID: s33582) and 3% lipofectamine RNAiMAX (Invitrogen) was incubated for 5 minutes at room temperature and an appropriate volume specified in the manufactures protocol was added to cells of interest. Medium was refreshed every 1 – 2 days. After 4 days, the cells were lysed or stained for analyses.

WESTERN BLOT

siCHD8 transfection efficiency was analysed by quantification of CHD8 protein expression using immunoblot analysis.

Samples were prepared by cell lysis whereby cells were exposed to radioimmunoprecipitation assay buffer with 0.1% protease inhibitor (cocktail set III; Merck, Calbiochem). Samples were collected and centrifuged, whereafter the supernatant was stored at -80°C. Protein concentrations of the samples were quantified by a detergent compatible (DC) protein assay (Bio-Rad, CA, USA) following the manufacturers protocol. With this colorimetric method, protein concentration was indicated by a reaction whereby protein reacts with Folin's reagent and alkaline copper tartrate to form a blue product. A spectrophotometer measured the colour intensity at a wavelength of 750 nm.

Proteins were separated based on molecular weight using a sodium dodecyl sulphate polyacrylamide gel electrophoresis (SDS-PAGE) whereby 10 µg protein per sample was loaded in a 4 – 12% gradient gel (Invitrogen). Subsequently, proteins were transferred to a polyvinylidene fluoride (PVDF) membrane (Bio-Rad, CA, USA), washed with tris buffered saline with 0.05% Tween-20 (TBS-T) and blocked with 5% w/v non-fat dry milk (Campina, NL) in TBS-T for 1 hour at room temperature. Thereafter, membranes were incubated overnight at 4°C with 1:5000 rabbit derived α-CHD8 (Cell Signalling Technology) and 1:5000 mouse derived α-tubulin (Abcam) and then incubated for 1 hour with 1:10,000 α-rabbit or α-mouse horseradish peroxidase conjugated secondary antibody (Promega, WI, USA). After washing with TBS-T, blots were visualized with a SuperSignal West Femto Chemiluminescent substrate kit (Thermo Fisher Scientific, MA, USA) and imaged using a FluorChem M imaging system (ProteinSimple, CA, USA). Results were quantified with ImageJ (version 1.53K, USA) using `Analyze → Gels`.

MEMBRANE FABRICATION

The BBB model consisted of a co-culture of astrocytes and endothelial cells, separated by a porous PDMS membrane. This membrane was fabricated and given to use for this research by Mariia Zakharova.

First, a sacrificial positive photoresist layer (AZ 9260, Fujifilm, Japan) was formed and deposited on a 525 µm thick silicon (Si) wafer (Okmetic, Finland) at 2000 rpm. The obtained film was incubated on a hot plate for 2 minutes at 110°C. A mask with 3 µm diameter pores was aligned with the wafer and exposed to UV at 12 mW^{-2} for 17 seconds using hard contact mode. After another 110°C incubation, the microcolumns were developed in an OPD4246 developer. Subsequently, columns were washed with de-ionized H_2O and a mixture of PDMS and curing agent (Sylgard 184 Silicone elastomer kit, Dow Corning) at a 10:1 w/w ratio was prepared. The PDMS was spin-coated over the microcolumns at 4000 rpm for 1 minute and incubated at 60°C for a minimum of 3 hours. Etching was performed using a reactive-ion etching system (TEtske, Nanolab University of Twente, The Netherlands) at 47 sccm SF_6 and 17 sccm O_2, 100 W, and 50 mTorr for 2 minutes.

CHIP FABRICATION

Chip design used in this research is shown in *figure 4*. The chip is made out of two compartments, whereby both contain a channel with a width of 500 µm and a height of 375 µm. The channels are perpendicular to each other, resulting in a cross section of 0.25 mm^2 with a PDMS membrane with 3 µm pores in between. Chips were made from PDMS mixed with curing agent at a 10:1 w/w ratio. After degassing in the desiccator, the mixture was poured over a SU-8 patterned silicon wafer, degassed again, and cured for minimal 4 hours at 60°C. Subsequently, the cured PDMS was removed from the wafer and the chips were cut and divided in top and bottom components. In the top compartment, 1.2 mm wide in- and outlets were punched. To bond the chip top component with the membrane containing silicon wafer, both were treated with oxygen plasma in a plasma oven, whereafter both parts were pressed together and incubated in 60°C for 10 minutes. Next, the top components with the attached wafer were submerged in acetone to remove the photoresist of the wafer, leaving the desired membrane. Next, the top and bottom components were treated with oxygen plasma and bonded together whereafter they were incubated at 60°C for 10 minutes.

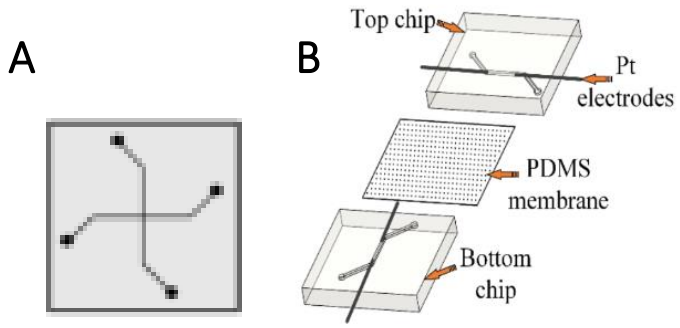

Figure 4: Schematic overview of the chip design used in this research. *A) Top view of chip (1.5 cm x 1.5 cm. B) Side view of chip compartments. Electrodes can be used for TEER measurements. Channel width is 500 µm and channel height is 375 µm.*

PERMEABILITY ASSAY

The integrity of an astrocyte co-cultured endothelial cell layer was analysed by measuring permeability. The assay was performed by tracking transport of fluorescently labelled dextran from the apical to the basolateral side of the membrane. The permeability assay was performed on transwells and chips, whereby the principle was the same.

To use the PDMS membrane for cell culture on transwells, the commercially derived membrane of the transwell insert (Corning, NY, USA) was removed and replaced by a 2 µm thick, 3 µm pore sized PDMS membrane. Uncured

PDMS with curing agent in a 10:1 w/w ratio was used as glue between the bottom rim of the insert and the silicon wafer with the membrane, which was cured at 60°C for 3 hours afterwards. The membrane was released from the silicon substrate by dissolving the silicon wafer with PDMS membrane in a 7:3 v/v ratio mixture of acetone and ethanol (100%). The transwell insert with PDMS membrane was sterilized by immersing in 70% ethanol v/v for 1 hour and subsequently exposed to oxygen plasma in a plasma oven (CUTE, Femto Science Inc., South Korea). Prior to cell seeding, membranes were washed 3 times with PBS.

At the start of the assay, 600 µL of fresh EGM was added to the bottom compartment and the medium of the top compartment was replaced by 100 µL fluorescein isothiocyanate (FITC)-dextran of a size of 20 or 40 kDa (Sigma Aldrich, Germany) in EGM at a concentration of 100 µg mL^{-1}. At the start and after 2, 5, 10, 15, 30, 45 and 60 minutes, 100 µL of medium was sampled from the bottom compartment and transferred to a black bottom 96-well plate (Corning, NY, USA). 100 µL of fresh medium was directly pipetted back to the bottom compartment to prevent pressure development over the membrane. Fluorescent intensity was measured using a Victor3 plate reader (PerkinElmer, Ma, USA) with an excitation and emission wavelength at respectively 485 and 528 nm. The values of the measured fluorescence intensity were converted to concentration (g mL^{-1}) using a calibration curve. Permeability of each membrane was calculated using:

$$P = \frac{1}{\text{Ia max}} \frac{V}{S} \frac{dIb}{dt} \left[\frac{cm}{s}\right]$$

Where P is the permeability in cm s^{-1}, $Ia\ max$ the maximum fluorescence intensity in the apical compartment (100 µg ml^{-1}), V the volume of the apical compartment (0.1 mL), S the area of the culture membrane (0.33 cm^2) and dIb/dt the slope of the intensity curve.

Results derived from the previous equation were normalized against blanco transwell membranes using the following formula:

$$\frac{1}{Pa} = \frac{1}{Pc} - \frac{1}{Pm} \left[\frac{cm}{s}\right]$$

Where Pa is the normalized permeability in cm s^{-1}, Pc the permeability measured of membranes with co-culture and Pm the permeability measured of membranes without cells.

LIVE/DEAD ASSAY

To determine the viability of cell culture on chip, a live/dead assay was performed using a Viability/Cytotoxicity kit (Invitrogen) containing calcein acetoxymethyl ester (Calcein-AM) and ethidium homodimer-1 (EthD-1). The non-fluorescent Calcein-AM becomes green fluorescent when linked to cytosolic esterases in living cells. EthD-1 becomes red fluorescent when it passes disrupted cell membranes and binds to DNA, which indicates dead cells. A solution of 1:60 Calcein-AM, 1:15 EthD-1 and one drop of Nucblue (Sigma Aldrich, Germany) in PBS was introduced in both channels of the chip and after 30 minutes of incubation, cells were imaged using an EVOS microscope (EVOS M5000, PA, USA) with an excitation and emission wavelength of respectively 528 and 617 nm. The two conditions that were analysed were hCMEC/D3 and astrocyte co-cultures with and without siCHD8 treatment.

STATISTICS

Graphs and statistical analyses were obtained using SPSS (IBM, version 28; Stanford, California, USA). P-values were obtained by using `Analyze → Descriptive Statistics → Explore`. $P \leq 0.05$ was considered statistically significant.

RESULTS AND EXPERIMENTAL DISCUSSION

SILENCING OF CHD8

Since a CHD8 suppressed BBB model is desired, transfection of siCHD8 was performed.

Since siCHD8 transfection in astrocytes with transfection reagent RNAiMAX has worked appropriately in previously, it was decided to repeat this for the ASD specific BBB model. Besides astrocytes treated with siCHD8, astrocytes treated with negative control silencer (siNC), RNAiMAX and astrocytes without treatment were taken along (*figure 5*).

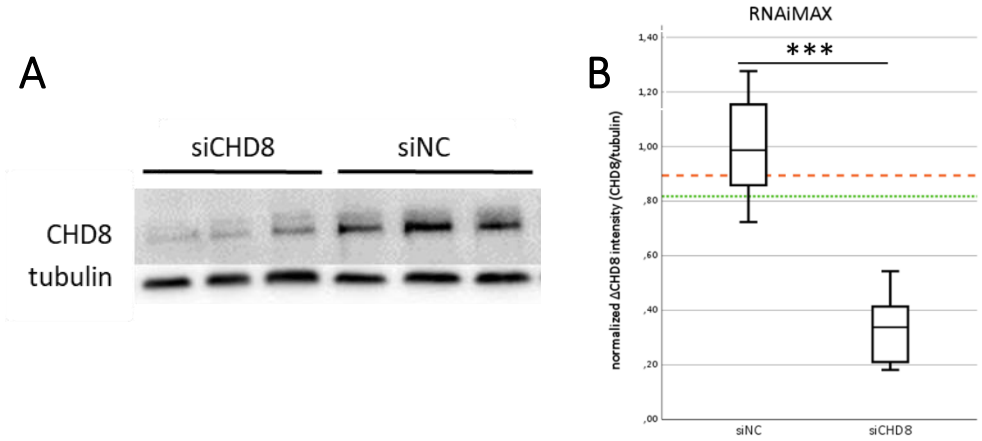

Figure 5: siCHD8 transfection in astrocytes using RNAiMAX. A) Representative image of a western blot showing CHD8 and tubulin protein bands after siCHD8 or siNC treatment (n = 3). B) Normalized ΔCHD8 intensity after siCHD8 (n = 8) or siNC (n = 8) treated astrocytes using RNAiMAX. Average CHD8 intensity in astrocytes after zero treatment (orange line; n = 8) and average CHD8 intensity in astrocytes after treatment with exclusively RNAiMAX (green line; n = 6) are also shown. $P < 0.05$.

CHD8 protein levels were successfully decreased in astrocytes after siCHD8 treatment using transfection reagent RNAiMAX. CHD8 protein levels were on average 3.02 times lower in astrocytes treated with siCHD8 than astrocytes treated with siNC. With a P-value of less than 0.05, the result is interpreted statistically significant.

The effectiveness of four types of transfection reagents were tested to optimize siCHD8 transfection in endothelial cells, namely RNAiMAX, Lipo2000, Viafect and Dharmafect. Besides hCMEC/D3 treated with siCHD8, hCMEC/D3 treated with siNC, transfection reagent, and hCMEC/D3 without treatment were analysed (*figure 6; appendix 2*).

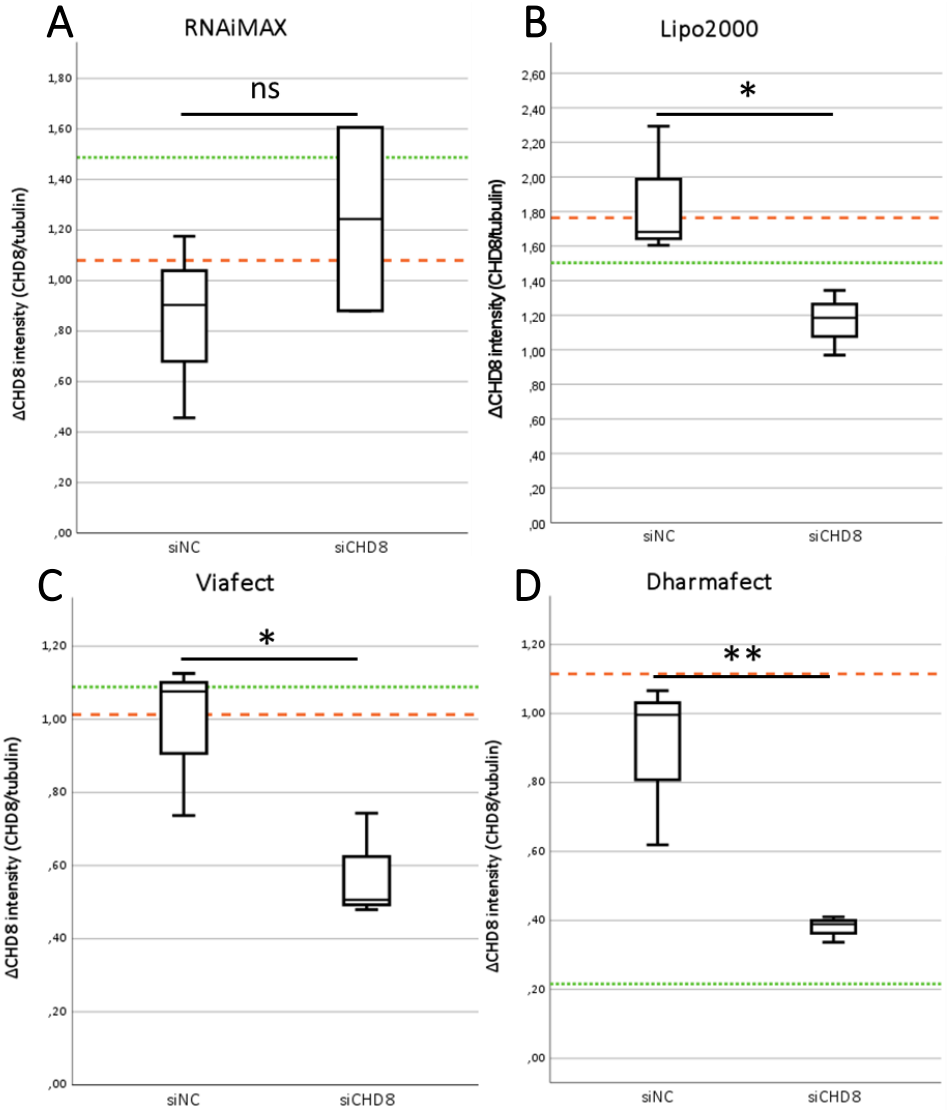

Figure 6: siCHD8 transfection in hCMEC/D3 using RNAiMAX, Lipo2000, Viafect and Dharmafect. ΔCHD8 intensity after siCHD8 or siNC treated hCMEC/D3 using A) RNAiMAX, B) Lipo2000, C) Viafect or D) Dharmavect. n = 3 for all boxplots, except for siCHD8 in A, which is n = 2. Average CHD8 intensity in hCMEC/D3 after zero treatment (orange line; n = 2) and average CHD8 intensity in hCMEC/D3 after treatment with exclusively transfection reagent (green line; n = 2) are also shown. *P < 0.2 and **P < 0.1

CHD8 protein levels did not decrease in hCMEC/D3 after siCHD8 treatment using transfection reagent RNAiMAX. The results indicate no potential for future use of RNAiMAX in efficient siCHD8 transfection in hCMEC/D3.

CHD8 protein levels did decrease in hCMEC/D3 after siCHD8 treatment using transfection reagent Lipo2000, Viafect, or Dharmafect. Respectively, CHD8 expression after siCHD8 treatment was 1.60 (P < 0.2), 1.70 (P < 0.2), and 2.36 (P < 0.1) times lower than in control treatment with siNC. With a p-value higher than 0.05, results cannot be considered statistically significant.

Furthermore, CHD8 intensity in hCMEC/D3 with exclusively Lipo2000 was slightly decreased compared to the negative controls, suggesting a negative effect of the transfection reagent on hCMEC/D3. Altogether, the results indicate that Lipo2000 is not an optimal transfection reagent for efficient siCHD8 transfection in hCMEC/D3. Both cells without treatment and treatment with extensively transfection reagent Viafect showed CHD8 expression retainence. Even though, decrease in CHD8 expression after silencing was not statistically significant, due to noticeable effectiveness and the small sample size taken into account, Viafect show potential for future use in efficient siCHD8 transfection in hCMEC/D3. A conspicuous low CHD8 expression was seen in hCMEC/D3 after treatment with exclusively Dharmafect. Even though, this raises questions on the effect of the transfection reagent upon hCMEC/D3, it was taken into account again that the sample size was too small to make definitive conclusions. Altogether, Dharmafect show potential for future use in efficient siCHD8 transfection in hCMEC/D3.

CO-CULTURE ON CHIPS

To transform a static BBB model to a dynamic one, chips were fabricated and seeded with a co-culture of hCMEC/D3 and astrocytes.

Chips were fabricated out of PDMS that was cured upon a patterned SU-8 mould. The cured PDMS was peeled of the mould and each chip compartment was separated by cutting. After punching in- and outlets in the top compartment, the top and bottom compartment were bonded together with a 2 µm thick 3 pore sized PDMS membrane in between (*figure 7*). Success rate of chip fabrication that was functional for co-culture was around 80%. Reason of rejecting 20% of the chips was mainly due to leakiness or channel clogging.

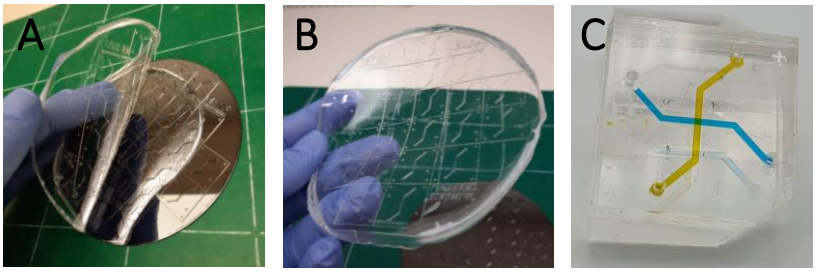

Figure 7: Fabrication of a PDMS chip. A and B) PDMS was cured upon a patterned SU-8 mould, resulting in 12 bottom comportments and 12 top compartments. After cutting each compartment and punching in- and outlets, the compartments are bonded together, C) resulting in a chip with two channels perpendicular to each other. Orange and blue colouring was used to indicate the channels clearly.

Astrocytes and hCMEC/D3 were seeded in the bottom and top channel, respectively. The co-culture was kept in culture for 4 – 5 days. Morphology of the co-culture in chip was observed with a microscope (*figure 8*).

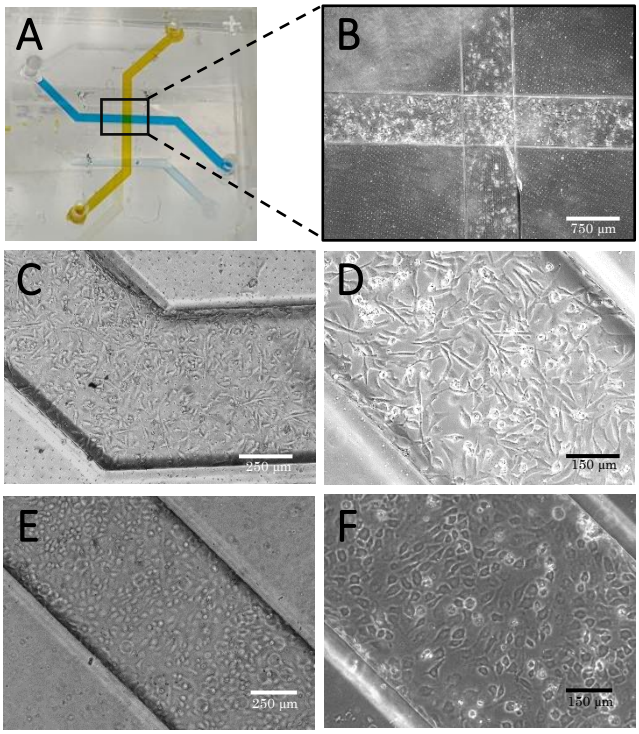

Figure 8: Co-culture in chip. A) Image of a chip (1.5 x 1.5 cm) without cells whereby the channels are indicated with colouring. B) Cross section of channels seeded with astrocytes (left to right) and hCMEC/D3 (top to bottom). C and D) Astrocytes at day 4 of cultivation. E and F) hCMEC/D3 at day 4 of cultivation.

After 5 days of cultivation in chip, a decent monolayer of hCMEC/D3 was observed. Both astrocytes and hCMEC/D3 appeared alive and were proliferating. At day 5, a live/dead assay was performed to confirm this observation (*figure 9*). Live and dead cells were respectively stained with Calcein-AM and EthD-1. DAPI was used to stain the nuclei. To also analyse damage to cells by siCHD8 transfection in chip, CHD8 silenced co-cultures were also included in the experiment.

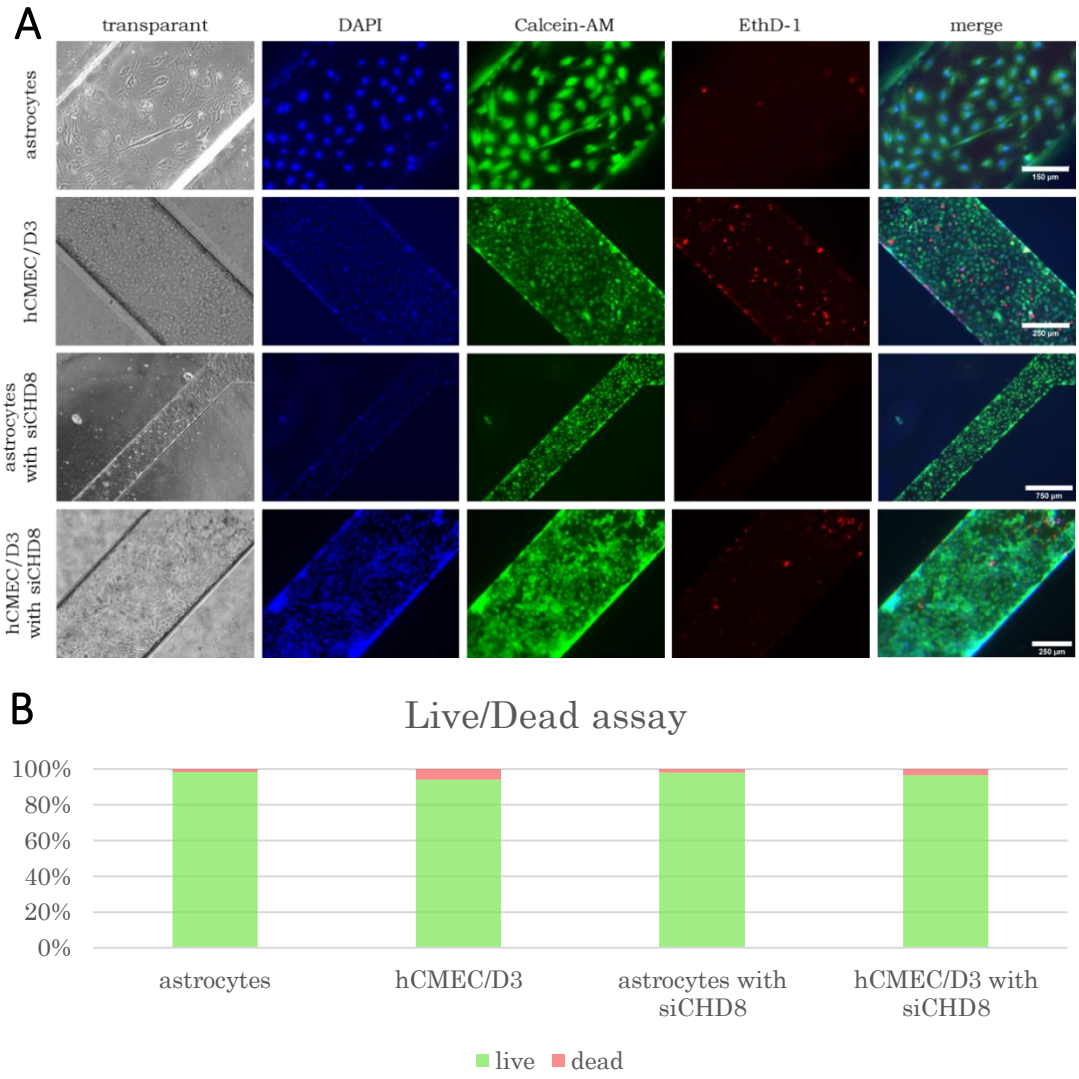

Figure 9: Live/dead assay on chip. A) Representative images of astrocytes and hCMEC/D3 with and without siCHD8 transfection. Living cells are stained with Calcein-AM (green), dead cells are stained using EthD-1 (red), and cell nuclei are stained with NucBlue (blue). B) Percentages of live (green) or dead (red) astrocytes and hCMEC/D3 with and without siCHD8 transfection (n = 3).

The viability for astrocytes (98.4 ± 0.4%), hCMEC/D3 (94.2 ± 1.3%), astrocytes with siCHD8 transfection (98.2 ± 0.7%), and hCMEC/D3 with siCHD8 transfection (96.5 ± 0.8%) was high. These results indicate that both the 5-day cell culture in chip and the siRNA transfection were not harmful to the cells.

PERMEABILITY ASSAY

To analyse cell layer integrity with and without siCHD8 transfection, a permeability assay on transwells was performed (*figure 10*).

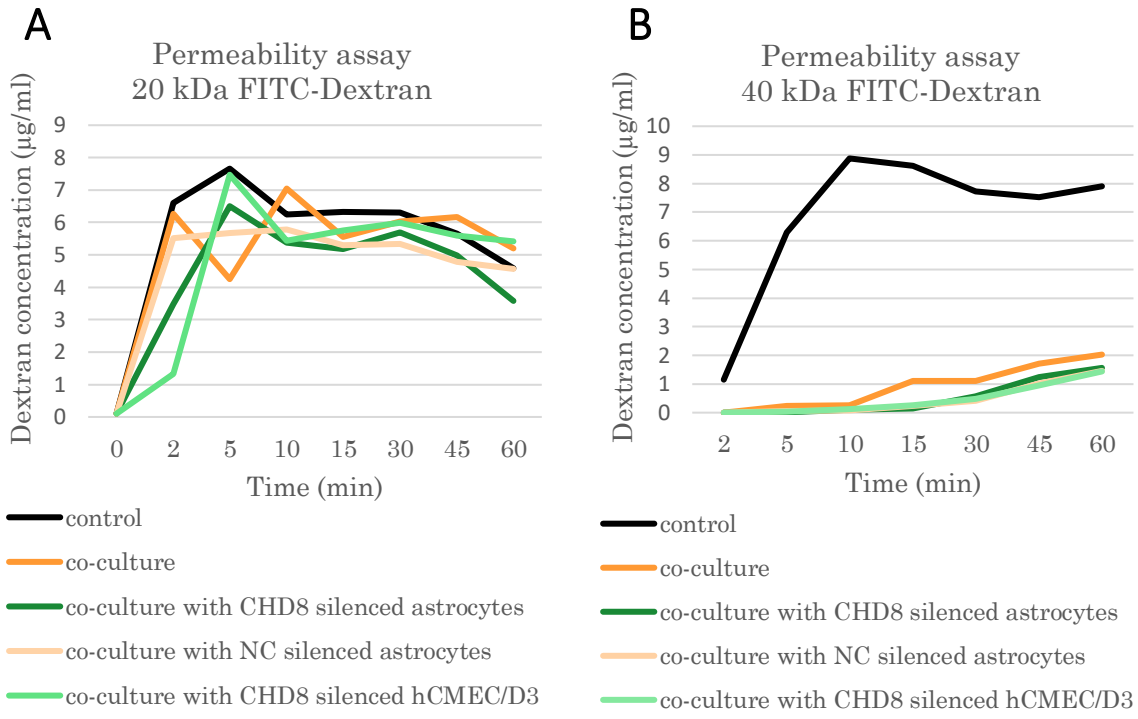

Figure 10: Permeability assay. Two separate permeability assay results on transwells with PC membranes, whereby A) 4 days of culture and 20 kDa FITC-Dextran and B) 7 days of culture and 40 kDa FITC-Dextran was used (n = 3).

The permeability assay in *figure 10A*, after 4 days of culture and using 20 kDa FITC-Dextran, was performed on polystyrene (PS) membranes. The results show that the co-cultured conditions had an average permeability of approximately $6.78 \cdot 10^{-2}$ cm s^{-1}. Since the permeability of the co-cultures is very high, it is concluded that a dense monolayer of hCMEC/D3 was not formed yet after 4 days of culture. Because of this, further conclusions between the different conditions cannot be drawn.

PS is known to be optically opaque, which made it difficult determining when the hCMEC/D3 monolayer was formed properly. To track monolayer formation in another permeability assay, shown in *figure 10B*, co-cultures on polyethylene terephthalate (PET) and PDMS membranes were seeded in parallel (*figure 11).*

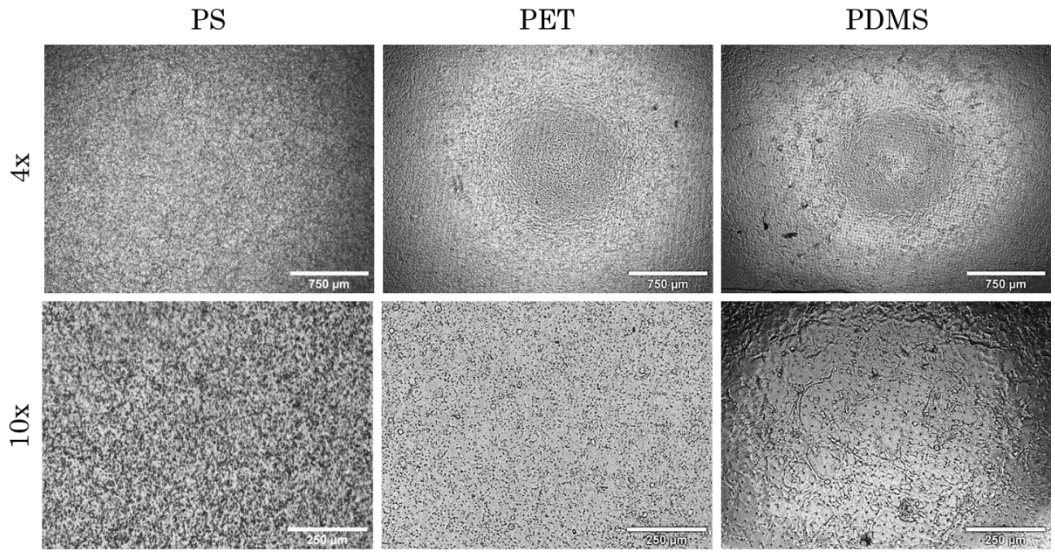

Figure 11: Phase-contrast images of PS, PET, and PDMS membranes with a co-culture of astrocytes and hCMEC/D3. *PS is opaque, PET is semi-transparent, and PDMS is transparent.*

A dense monolayer was observed after 7 days of culture. To prevent an untrackable fast transport across the monolayer, a higher molecular weight of 40 kDa FITC-Dextran was used. The results show that all co-culture conditions have a lower permeability (average of $3.21 \cdot 10^{-3}$ cm s^{-1}) than compared to the membrane without cells, concluding that the hCMEC/D3 monolayer formed an integer barrier after 7 days of culture. However, due to limited transport of FITC-Dextran across the monolayer, differences between conditions are too small to draw further conclusions.

DISCUSSION

In this research, a CHD8 suppressed human BBB model on chip for ASD specific analysation of BBB permeability was optimized, due to an increased CHD8 silencing efficiency, creation of an integer hCMEC/D3 monolayer functioning as barrier, and establishment of a viable co-culture on chips. However, it must be taken into account that not all characteristics of the BBB *in vivo* are met.

BBB CELL ORGANIZATION

Multiple studies suggest that all cell types of the neurovascular unit contribute to *in vivo* BBB functionality, while the BBB model used in this research only consists of astrocytes and endothelial cells. [6, 9, 53, 55] Pericytes are the most frequently mentioned, which are essential for BBB regulation during formation and maintenance. [17, 57, 58] Studies also report the important communicative role of pericytes between other cells of the neurovascular unit and that without these, the BBB becomes vulnerable. [17, 59] For instance, M. A. Mäe *et al.* (2021) shows that pericyte deficiency changes identity and behaviour of BECs with degradation of BBB integrity as a result, and J. Keaney and M. Campbell (2015) indicates that the BBB is not just an impermeable wall, but should rather be seen as a communication centre in which all cell types, including pericytes, contribute to proper BBB functioning. [15, 57] In practice, this can result in a chip that S. I. Ahn *et al.* (2020) shows, in which a channel for pericyte cultivation is parallelly integrated next to the astrocyte containing channel. Both channels are in contact with the top channel, separated by a porous membrane. [60] Inclusion of pericytes, or even neurons or microglia in the BBB model will increase physiological accuracy and thereby predictive potential. However, as mentioned before, increased physiological accuracy is directly associated with increased technical complexity. Every addition to the model must be carefully considered whether the benefits of addition outweigh the associated increased complexity. [55] This research focuses on CHD8 associated BBB permeability in ASD diagnosed children. Because CHD8 expression in pericytes manifest only in adulthood, addition of pericytes has minimal added value in the BBB model for this research. [33]

Another point to keep in mind, is that the endothelial cell line hCMEC/D3 used in this research, is not equal to human BECs, with the fundamental difference that the first mentioned is immortalized. However, hCMEC/D3 has become widely used as a model for the human BBB due to their contact-inhibited monolayer and expression of BBB characteristic adherens and tight junction proteins in culture. Nevertheless, it has been shown that the expression level of claudin-5, important for junctional tightness, is lower than in *in vivo* conditions. [61, 62] Subsequently, E. A. L. M. Biemans *et al.* (2016) shows that hCMEC/D3 form a decent barrier for molecules with a high molecular weight,

but is less efficient to inhibit small molecules to permeate, suggesting that the incomplete claudin-5 expression plays an important role in barrier integrity. [62] On the other hand, studies show that this issue is partially addressed by addition of astrocytes and/or pericytes and physiological shear stress that increases junctional tightness and decreases permeability *in vitro.* [61, 62] All together, the hCMEC/D3 cell line makes an easy to use, BBB characteristic model of human origin and is, co-cultured with astrocytes, very well suited for this research.

ENVIRONMENTAL FACTORS OF THE BBB

Although not utilized in this research, an advantage of a microfluidic chip over a static transwell is that it is able to implement flow. Flow-induced shear stress play an important role in BBB functionality as it is proven to increase expression of tight junction proteins in BECs and enhance barrier integrity. [55, 63, 64] To mimic physiological conditions of brain capillaries, a shear stress of 0.3 – 2 Pa should be implemented. [53] Using the equation for determination of shear stress in rectangular channels cited in *appendix 1,* it is calculated that a flow of 285.5 μL min^{-1} must be achieved to create a minimal shear stress of 0.3 Pa in the chip used in this research. Given maximum flow rates used in other equivalent studies, achieving such flow rate will be challenging. [53, 65, 66] However, adapting the channel in such a way that the width is much larger than the height (w >> h), the same shear stress could be obtained with a lower flow rate. [53, 67] In further research, flow induced shear stress will contribute to BBB model optimalization.

As mentioned before, the neurovascular unit should be seen as a communication centre altogether in which cell-to-cell contact and anatomical organization are environmental factors for proper BBB functioning. [15, 57] Both in the transwell as in the chip, astrocytes and hCMEC/D3 were cultured in 2D on opposite sides of a membrane, which does not match *in vivo* organization of brain capillaries, in which astrocyte end-feed totally surround cylindrical shaped endothelial cells. [55, 63] It is important to keep in mind that results of a 2D co-culture cannot be translated to *in vivo* situations one to one.

ASD ASSOCIATED GENE MUTATION

Since CHD8 is important in brain development and is designated as main contributor for ASD development when mutated, it is logical that focus is on this gene in the ASD specific BBB model. [41, 42] However, it will also be interesting to study expression of CHD7 and mechanics between CHD8 and CHD7, since they are in close interaction with each other. Furthermore, M. Coll-Tané *et al.* (2021) shows a high expression of both CHD8 and CHD7 in neurovascular unit cells, suggesting that besides CHD8, CHD7 also plays an essential role in the BBB. [33] In future research, it would be interesting to

analyse CHD7 expression and interactions between CHD8 and CHD7 for improved understanding of the mechanisms underlying sleep problems in ASD diagnosed children. [33, 38, 39]

RECOMMENDATIONS

For proper CHD8 suppression in the BBB model, both astrocytes and hCMEC/D3 should be efficiently silenced. Since silencing of hCMEC/D3 using Viafect and Dharmafect gave promising, but not yet significant results, it is recommended to optimize silencing conditions, focussing on siCHD8/reagent ratio and incubation time.

Since only a limited amount of 40 kDa FITC-Dextran passed the hCMEC/D3 monolayer within 60 minutes during the permeability assay on transwell, it is recommended to use molecules with different molecular weight and fluorescent tag. In this way, barrier permeability can be analysed for both small and large molecules at the same time.

Furthermore, it is recommended to analyse hCMEC/D3 monolayer integrity on chip by also performing a permeability assay with FITC-Dextran. FITC-Dextran transport across the membrane can be determined by measuring fluorescent intensity in the bottom channel after inserting FITC-Dextran in the top one. A first try-out of such an experiment was performed on one chip (*figure 12*). The chip was not fixed in one place during the experiment, which is recommended when doing this properly.

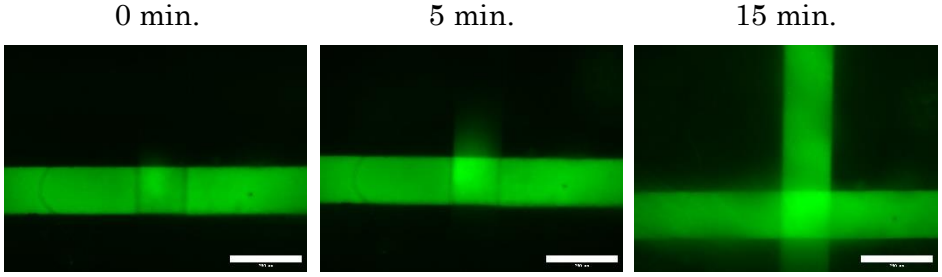

Figure 12: Representative fluorescent images of FITC-Dextran transport in chip. *Try out of permeability assay on chip, whereby FITC-Dextran was inserted in the top channel and fluorescent intensity was observed in the bottom channel at the start and after 5 and 15 minutes incubation. Scale bar is 750 µm.*

Since CHD8 suppression in the BBB model is of major importance, it would be convenient to trace CHD8 in chip by immunofluorescence. In this way, silencing efficiency could be measured by comparing fluorescent intensities in different conditions.

To increase BEC specific characteristics in hCMEC/D3, flow should be implemented to create shear stress of 0.3 – 2.0 Pa. To achieve this, it is recommended to alter the chip design in such a way that the width >> height.

CONCLUSION

The aim of this research was to optimize a CHD8 suppressed human BBB model for examination of barrier integrity in ASD diagnosed children with sleep problems.

CHD8 was successfully suppressed in astrocytes with transfection reagent RNAiMAX, while suppression in hCMEC/D3 showed promising results with transfection reagents Viafect and Dharmafect. An integer barrier with low permeability was formed by a hCMEC/D3 monolayer co-cultured with astrocytes after 7 days of cultivation. However, no conclusion in permeability difference could be drawn between CHD8 suppressed co-cultures and cultures without treatment. Furthermore, hCMEC/D3 and astrocyte co-culture was viable in PDMS chips after 4 days of cultivation.

In conclusion, this research optimized a CHD8 suppressed human BBB model, by increasing CHD8 silencing efficiency, creating an integer co-culture barrier, and making a first step transforming a static transwell to a dynamic chip.

ACKNOWLEDGEMENTS

I would like to thank my daily supervisor Robin Pampiermole, by whom I could literally turn to daily for experimental and theoretical questions when needed and often helped me out on the lab. Also, I would like to thank Prof. Dr. Ir. Loes Segerink and Dr. Kerensa Broersen for their positive, yet critical feedback during our meetings.

Furthermore, I would like to thank Mariia Zakharova for receiving the PDMS membranes and borrowing multiple stuff more, Jolien Wichers Scheur for helping me fabricating my very first chips, Ing. Carla Annink, who had to help me on the lab more frequently than intended, Laura and Gerben for providing me transfection reagents, and Tonnie Baumeister for an experimental set up improvement.

Last but not least, I would like to thank my fellow students and BIOS members for creating such a pleasant atmosphere to work in!

REFERENCES

[1] J. Stiles and T. L. Jernigan (2010) "The Basics of Brain Development" *Neurophysiology Review,* Volume 20, Issue 4, pages 327 – 348

[2] A. Pascual-Leone and R. Hamilton (2001) "The metamodel organization of the brain" *Progress in Brain Research,* Volume 134

[3] G. Fricker, M. Ott and A. Mahringer (2016) *Topics in Medicinal Chemistry: The Blood Brain Barrier (BBB),* Springer, USA.

[4] Image taken from: https://brainbarriers4you.eu/bbbmouse_en.html at 18 - 05 – 2022

[5] Y. Liang and J. Yoon (2021) "*In situ* sensors for blood-brain barrier (BBB) on a chip" *Sensors and Actuators Reports,* Volume 3

[6] L. Jena *et al.* (2020) "Delivery across the blood-brain barrier: nanomedicine for glioblastoma multiforme" *Drug Delivery and Translation Research,* Volume 10, Issue 2, pages 304 – 318

[7] S. Nag (2011) *The Blood-Brain and Other Neural Barriers; Methods in Molecular Biology*. Springer Protocols, UK

[8] J. Doh, D. Fletcher and M. Piel (2018) *Microfluidics in Cell Biology Part A: Microfluidics for Multicellular Systems; Chapter 9 – Blood-brain barrier on a chip*. Elsevier, Amsterdam, The Netherlands.

[9] M. M. A. Almutairi *et al.* (2015) "Factors controlling permeability of the blood-brain barrier" *Cellular and Molecular Life Sciences*

[10] S. Liebner *et al.* (2018) "Functional morphology of the blood-brain barrier in health and disease" *Acta Neurophatlogica,* Volume135, pages 311 – 336

[11] M. B. Chancellor *et al.* (2012) "Blood-Brain Barrier Permeation and Efflux Exclusion of Anticholinergics Used in the Treatment of Overactive Bladder" *Drugs Aging,* Volume 29, Issue 4, pages 259 – 273

[12] P. Ballabh *et al.* (2004) "The blood–brain barrier: an overview Structure, regulation, and clinical implications" *Neurobiology of Disease,* Volume 16, Issue 1, pages 1 – 13

[13] M. Corada *et al.* (2001) "Monoclonal antibodies directed to different regions of vascular endothelial cadherin extracellular domain affect adhesion and clustering of the protein and modulate endothelial permeability" *Blood,* Volume 97, Issue 6, pages 1689 – 1684

[14] R. Pandit *et al.* (2019) "The blood-brain barrier: Physiology and strategies for drug delivery" *Advanced Drug Delivery Reviews*

[15] W. Jiang (2013) "The role of claudin-5 in blood-brain barrier (BBB) and brain metastases" *Molecular Medicine Reports*

[16] J. Keaney and M. Campbell (2015) "The dynamic blood-brain barrier" *FEBS J,* Volume 282, Issue 21, pages 4067 – 4079

[17] E. S. Lippmann *et al.* (2013) "Human Blood-Brain Barrier Endothelial Cells Derived from Pluripotent Stem Cells" *Nature Biotechnology*, Volume 30, Issue 8, pages 783 – 791

[18] An. Quaegebeur *et al.* (2010) "Pericytes: Blood-Brain Barrier Safeguards against Neurodegeneration?" *Neuron,* Volume 68, pages 321 – 323

[19] R. D. Bell *et al.* (2010) "Pericytes control key neurovascular functions and neuronal phenotype in the adult brain and during brain aging" *Neuron,* Volume 68, Issue 3, pages 409 – 427

[20] N. L. Stone *et al.* (2019) "A Novel Transwell Blood Brain Barrier Model Using Primary Human Cells" *Frontiers in Cellular Neuroscience*

[21] M. Zakharova *et al.* (2021) "Transwell-Integrated 2 μm Thick Transparent Polydimethylsiloxane Membranes with Controlled Pore Sizes and Distribution to Model the Blood-Brain Barrier" *Advanced Materials Technologies*

[22] C. Kuo and S. Majd (2020) "An Improved in Vitro Blood-Brain Barrier Model for Applications in Therapeutics' Delivery to Brain" *Engineering in Medicine and Biology*

[23] H. C. Helms *et al.* (2016) "In vitro models of the blood-brain barrier: An overview of commonly used brain endothelial cell culture models and guidelines for their use" *Journal of Cerebral Blood Flow & Metabolism,* Volume 36, Issue 5, pages 862 – 890

[24] K. Francis *et al.* (2003) "Innate immunity and brain inflammation: the key role of complement" *Expert Reviews in Molecular Medicine,* Volume 5, Issue 15

[25] F. Chiarotti and A. Venerosi (2020) "Epidemiology of Autism Spectrum Disorders: A Review of Worldwide Prevalence Estimates Since 2014" *Brain Sciences*; Volume 10

[26] L. Campisi *et al.* (2018) "Autism spectrum disorder" *British Medical Bulletin,* Volume 127, Issue 1, pages 91 – 100

[27] K. Lyall *et al.* (2017) "The Changing Epidemiology of Autism Spectrum Disorders" *The Annual Review of Public Health*

[28] H. Hodges *et al.* (2019) "autism spectrum disorder: definition, epidemiology, causes, and clinical evaluation" *Translational Paediatrics*

[29] C. Lord *et al.* (2018) "Autism spectrum disorder" *The Lancet,* Volume 392, Issue 10146, pages 508 – 520

[30] A. L. Richdale and K. A. Schreck (2009) "Sleep problems in autism spectrum disorders: Prevalence, nature, & possible biopsychosocial aetiologies" *Sleep Medicine Reviews,* Volume 13, Issue 6, pages 403 – 411

[31] B. Sivertsen *et al.* (2011) "Sleep problems in children with autism spectrum problems: a longitudinal population-based study" *Autism,* Volume 16, Issue 2, pages 139 – 150

[32] F. Waters *et al.* (2018) "Severe Sleep Deprivation Causes Hallucinations and a Gradual Progression Toward Psychosis With Increasing Time Awake" *Frontiers in Psychiatry,* Volume 9

[33] M. Coll-Tané *et al.* (2021) "The CHD8/CHD7/Kismet family links blood-brain barrier glia and serotonin to ASD-associated sleep defects" *Science Advances*

[34] A. M. Shui *et al.* (2018) "Predicting sleep problems in children with autism spectrum disorders" *Research in Developmental Disabilities,* Volume 83, pages 270 – 279

[35] P. H. Finan *et al.* (2013) "The association of sleep and pain: an update and a path forward" *The Journal of Pain,* Volume 14, Issue 12, pages 1539 – 1552

[36] C. A. Martin *et al.* (2019) "Associations between parenting stress, parent mental health and child sleep problems for children with ADHD and ASD: Systematic review" *Research in Developmental Disabilities,* Volume 93

[37] A. Levin and A. Scher (2016) "Sleep Problems in Young Children with Autism Spectrum Disorders: A Study of Parenting Stress, Mothers' Sleep-Related Cognitions, and Bedtime Behaviors" CNS *Neuroscience & Therapeutics,* Volume 22, Issue 11, pages 921 – 927

[38] R. K Earl *et al.* (2021) "Sleep Problems in Children with ASD and Gene Disrupting Mutations" *The Journal of Genetic Psychology*

[39] M. O. Mazurek *et al.* (2019) "Course and Predictors of Sleep and Co-occurring Problems in Children with Autism Spectrum Disorder" *Journal of Autism and Developmental Disorders*

[40] A. Robinson-Shelton and B. A. Malow (2016) "Sleep Disturbances in Neurodevelopmental Disorders" *Current Psychiatry Reports,* Volume 18, Issue 6

[41] R. Grzadzinski *et al.* (2016) "Parent-reported and clinician-observed autism spectrum disorder (ASD) symptoms in children with attention deficit/hyperactivity disorder (ADHD): implications for practice under DSM-5" *Molecular Autism*

[42] R. Bernier *et al.* (2014) "Disruptive CHD8 Mutations Define a Subtype of Autism Early in Development" *Cell,* Volume 158, Issue 2, pages 263 – 276

[43] O. Durak *et al.* (2016) "Chd8 mediates cortical neurogenesis via transcriptional regulation of cell cycle and Wnt signalling" *Nature Neuroscience,* Volume 19, Issue 11

[44] S. R. Lalani *et al.* (2009) "CHARGE syndrome" *GeneReviews*

[45] T. S. Hartshorne *et al.* (2005) "Autistic-like behavior in CHARGE syndrome" *Journal of Medical Genetics*

[46] R. Mittal *et al.* (2018) "Organ-on-chip models: Implications in drug discovery and clinical applications" *Journal of Cellular Physiology,* Volume 2019, Issue 234, pages 8352 – 8380

[47] R. Mittal *et al.* (2018) "Organ-on-chip models: Implications in drug discovery and clinical applications" *Journal of Cellular Physiology*

[48] J. Zhu (2020) "Application of Organ-on-Chip in Drug Discovery" *Journal of Biosciences and Medicines,* Volume 8, pages 119 – 134

[50] M. Zakharova *et al.* (2020) "Multiplexed blood-brain barrier organ-on-chip" *Lab on a chip,* Volume 20, Issue 17

[51] K. Raj M and S. Chakraborty (2019) "PDMS microfluidics: A mini review" *Journal of Applied Polymer Science*

[52] W. A. Banks *et al.* (2021) "Healthy aging and the blood-brain barrier" *Nature Aging,* Volume 1, Issue 3, pages 243 – 254

[53] M. W. van der Helm *et al.* (2016) "Microfluidic organ-on-chip technology for blood-brain barrier research" *Tissue Barriers,* Volume 4, Issue 1

[54] H. Leblochova "Transport of ion channel blockers across the blood-brain barrier in vitro" Master's thesis, 2010

[55] M. E. Katt and E. V. Shusta (2020) " In vitro models of the blood-brain barrier: building in physiological complexity" *Current Opinion in Chemical Engineering,* Volume 30, pages 42 – 52

[56] B. Weksler *et al.* (2013) "The hCMEC/D3 cell line as a model of the human blood brain barrier" *Fluids and Barriers of the CNS,* Volume 10

[57] M. A. Mäe *et al.* (2020) "Single-Cell Analysis of Blood-Brain Barrier Response to Pericyte Loss" *Circulation Research,* Volume 128, Issue 4

[58] S. I. Ahn and Y. Kim (2021) "Human Blood-Brain Barrier on a Chip: Featuring Unique Multicellular Cooperation in Pathophysiology" *Trends Biotechnology,* Volume 39, Issue 8, pages 749 – 752

[59] R. Daneman and A. Prat (2015) *The Blood-Brain Barrier,* Cold Spring Harbor Perspectives in Biology, Cold Spring Harbor Laboratory Press

[60] S. I. Ahn *et al.* (2020) "Microengineered human blood-brain barrier platform for understanding nanoparticle transport mechanisms" *Nature Communications,* Volume 11, Issue 175

[61] R. N. Gunn *et al.* (2012) "Combining PET biodistribution and equilibrium dialysis assays to assess the free brain concentration and BBB transport of CNS drugs" *Journal of Cerebral Blood Flow & Metabolism,* Volume 32, pages 874 – 883

[62] J. D. Wang *et al.* (2016) "Organization of Endothelial Cells, Pericytes, and Astrocytes into a 3D Microfluidic *in Vitro* Model of the Blood-Brain Barrier" *Molecular Pharmaceutics,* Volume 13, Issue 3, pages 895 – 906

[63] E. A. L. M. Biemans *et al.* (2016) "Limitations of the hCMEC/D3 cell line as a model for Aß clearance by the human blood-brain barrier" *Journal of Neuroscience Research*

[64] B. Elbakary and R. K. S. Badhan (2020) "A dynamic perfusion based blood-brain barrier model for cytotoxicity testing and drug permeation" *Scientific Reports,* Volume 10

[65] H. Gong *et al.* (2016) "High density 3D printed microfluidic valves, pumps, and multiplexers" *Lab on a Chip*

[66] J. Xiang *et al.* (2016) "A Micro-cam Actuated Linear Peristaltic Pump For Microfluidic Applications" *Sensors and Actuators A: Physical*

[67] Y. Son (2007) "Determination of shear viscosity and shear rate from pressure drop and flow rate relationship in a rectangular channel" Volume 48, Issue 2, pages 632 – 637

APPENDIXES

APPENDIX 1

Shear stress in rectangular channels can be calculated using the following equation:

$$\tau = \frac{6 \cdot \mu \cdot Q}{w \cdot h^2} \cdot \left(1 + \frac{h}{w}\right) \cdot f^* \left(\frac{h}{w}\right) [Pa]$$

In which τ is shear stress in Pa, μ is viscosity of the fluid in the channel in Pa•s, Q is volumetric flow rate in $m^3\ s^{-1}$, w is the width of the channel in m, h is the height of the channel in m, and the function $f^*(x)$ is an infinite summation series of which the output value depends on the height-width ratio of the channel and is stated in the article of Younggon Son (2007). [67] To calculate what flow rate is required for the desired shear stress, the equation is rewritten like this:

$$Q = \frac{\tau \cdot h^2 \cdot w^2 \cdot 10^{10}}{\mu \cdot f^* \left(\frac{h}{w}\right) \cdot (h + w)} [\mu L\ min^{-1}]$$

APPENDIX 2

Western Blot results using transfection reagent Viafect.

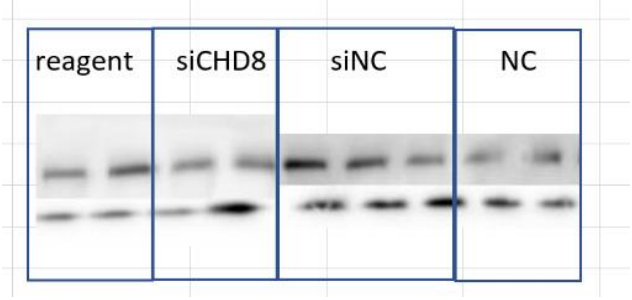

Western Blot results using transfection reagent RNAiMAX.

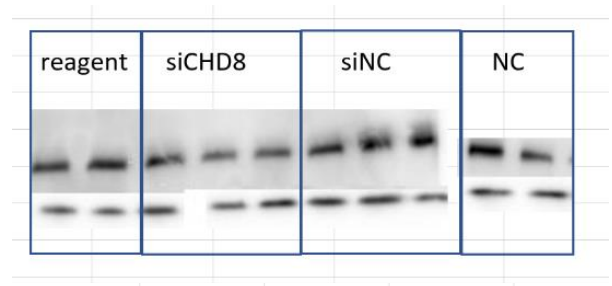

Western Blot results using transfection reagent Lipo2000.

Western Blot results using transfection reagent Dharmafect.